SCIREA Journal of Physics
ISSN: 2706-8862
http://www.scirea.org/journal/Physics
April 17, 2023
Volume 8, Issue 2, April 2023
https://doi.org/10.54647/physics140541

MXene-based material optimized shielding effectiveness of chassis

Ke Meng[1,*], Enbo Liu[1]

[1] Institute of Electromagnetic Compatibility, Guangzhou GRG Metrology & Test Co., Ltd, Guangzhou, China

*Corresponding author: LinnerMeng@Gmail.com

Abstract

The electronic equipment needs a special circuit design during working in complex electromagnetic environmental. Human-made or natural electromagnetic interference has a large effect on electronics. Both the couple of signal cable and the bit error rate during high-speed communication affects the reliability of equipment. Thus, electronic equipment with these problems is bad for the process of industrial production. Electromagnetic shielding is a good method to improve the radiated susceptibility of electronic equipment. The material of the chassis, the structure of chassis, and the thickness of the chassis wall affect the shielding effectiveness of chassis. Thus, in order to investigate the effect of microwave absorption material on the shielding effectiveness of chassis. This article is based on the material of the chassis, combing the simulation of High Frequency Structure Simulation (HFSS) software, to study the effect of MXene-based microwave absorption material on the shielding effectiveness. The simulation results indicate that chassis optimized by MXene-based materials has a better shielding effectiveness. When the thickness of the microwave absorption material is 0.6 mm, it shows a good shielding effectiveness.

Keywords: *Shielding Effectiveness, MXene, HFSS, Microwave absorption material*

1. Introduction

Wireless communication shrinks the information time cost between the space and the land, the land and the other land. 2020 is the first year of fifth-generation mobile communication. The widely used 5G communication technology makes virtual reality and autonomous vehicles perform a new appearance [1-4]. The intact of communication link covers the driver, the communication channel, and the receiver. Different communication systems are made of aforementioned these different three parts. Since communication systems are used to guarantee normal communication, the quality of signal is the main factor to assess the pros and cons of communication. The realization of low bit error rate, high traffic transmission, and low power consumption of communication systems could promote the development of society. There are many factors to influence the bit error rate, such as crosstalk, ringing, reflection, and timing jitter. The signal could accomplish the zero-bit error rate transmission ideally. However, the electric signal is easily to interrupted by external electromagnetic interference during the transmission in the communication channel. Finally, the signal is distorted [5]. What's more, the long-time transmission of electric signal could also decrease the signal power. This is because of the dielectric loss of the channel. When the electric signal has low power, it is also easily interrupted by the near high-power electric signal. The common channel could divide into two parts. One is free space, and the other one is a fiber or cable-based channel. Different communication channels have different mathematical model [6]. Electromagnetic interference could access the circuit through the coupling of the space. How to effectively decrease the interruption of electromagnetic interference to electronic equipment is urgent.

Oliver Heaviside published an article named "On interference" in 1881. This article first caught the researcher's attention about electromagnetic interference [7]. With the outbreak of World War II, the army became increasingly interested in radio communications. How to avoid the impact of electromagnetic disturbance on the communication system and ensure normal wartime communication was an urgent problem that needed to be solved at that time. Faraday Cage provides a feasible idea to isolate the interference in the system [8]. The completely enclosed metal chassis effectively shields electromagnetic disturbances from the metal material. As we all know, shielding, filtering, and grounding could effectively decrease

the problem of electromagnetic compatibility [9]. The shielding effectiveness of equipment will affect the use of electronic equipment directionally. The shielding effectiveness is mainly affected by the structure and material properties of the equipment shell [10].

Two-dimensional graphene materials have good wave absorption properties, and MXene with similar layered structures also has good wave absorption properties [11]. MXene films were successfully prepared from MAX by Yury Gototsi et al. in 2011 [12]. The chemical formula of MAX is $M_{n+1}AX_n$ (n=1, 2, 3), where M represents transition metal elements, A is group IIIA or group IVA elements (such as aluminum, gallium, silicon, germanium), and X is carbon or nitrogen. The chemical bond energy between the transition metal element and the carbon or nitrogen element in the MAX phase is large, and the bond energy with the IIIA or IA group elements is weaker. Thus, A is more likely to be stripped away under the reaction of the outside world to form MXene. The chemical formula of MXene is $M_{n+1}X_nT_x$ (n=1, 2, 3). Since the MXene is the reaction product of MAX, thus, the symbolic meaning of M, X is same as the MAX. -ene stands for olefin-type carbon-carbon double bond structure [13]; T represents the functional group, such as -O, -OH, -F; The subscript x represents the proportional of these functional group [14]. MXene possesses good electric, mechanics, antibacterial, photocatalysis, electrocatalysis, and supercapacitor properties [15-20]. MXene's potential in absorbing electricmagnetic wave is mainly reflected in the following three points: (1) The layer structure is adjustable, the distance between layer is also adjustable. This property could control the propagation trace of electromagnetic wave; (2) The conductivity of MXene-based materials up to $1.4 \pm 0.077 \times 10^6$ S/m. Such a high conductivity could accomplish the high dielectric loss and electric polarization loss [21]; (3) Since the abundant ionizing functional group of the surface of MXene, it is easy to form defect dipole; The defect dipole will orient with the external direction of the electric field, finally, it causes electric polarization loss [22]; (4) The transition metal elements contained in MXene, such as Fe, Co, Ni, Cr, and Mn, could also cause the magnetic loss [23]. What's more, since the microwave absorption effect of MXene, it is necessary to consider the impedance match during the practice using.

According to the transmission line theory, the impedance mismatch could cause the reflection of electromagnetic wave. The reflection loss (RL) can be calculated as follows:

$$RL = 20lg\left|\frac{Z_{in} - Z_0}{Z_{in} + Z_0}\right|$$

$$Z_{in} = Z_0 \sqrt{\frac{\mu_r}{\varepsilon_r}} \tanh\left[j\frac{2\pi f d}{c}\sqrt{\varepsilon_r u_r}\right]$$

Z_{in} is the input impedance; Z_0 is the characteristic impedance (50 Ω for communication, 377 Ω for free space); d is the thickness of dielectric material; c is the speed of light. Usually, when the $RL \leq -10dB$, this means the absorption material accomplished the 90% wave absorption. When $Z_{in}/Z_0 \approx 1$, the incident wave can be fully absorbed [24]. Thus, it is necessary to consider the impedance match of MXene during use in order to absorb the electromagnetic wave power.

Considering the above factors, Luyang Liang et al. successively prepared composite materials composed of (1) $Ti_3C_2T_x$ and Ni, (2) $Ti_3C_2T_x$, Ni and reduced graphene oxide, both of which can achieve better absorption performance, but the absorbing materials compounded with reduced graphene oxide can achieve 99.9999996% absorption performance [2, 26]. As mentioned earlier, the shielding effectiveness of the equipment is determined by the structure of the equipment and the material of the equipment; Since the above materials can achieve high absorbing performance, it must also be feasible to use this material to optimize the shielding performance of the chassis. Since the current large-area MXene synthesis process is not yet mature, this article uses MXene-based material, combing with HFSS software, to simulate and optimize the shielding performance of the chassis.

2. Simulation and Analysis

HFSS is Ansys' electromagnetic simulation software; Basing on the finite element method, the software can accurately obtain the electromagnetic field distribution on the surface and inside the chassis under high frequency conditions. It is a benchmark in the field of electromagnetic industry. It is well known that the behavior of electromagnetic waves can be described by the Maxwell equation; When electromagnetic waves enter a loss medium, the incident waves produce reflected waves as well as transmitted waves. The dielectric loss of the dielectric and the magnetic loss of the medium are the two main parts of attenuating electromagnetic waves [24, 27, 28]. The complex permittivity (ε_r) and complex permeability (μ_r) of the medium are as follows:

$$\varepsilon_r = \varepsilon' - j\varepsilon''$$
$$\mu_r = \mu' - j\mu''$$

Among them, ε', μ' are related to the energy storage of the field; ε''、μ'' are related to the energy dissipation of the field [29, 30]; Dielectric loss and magnetic loss can be defined by the above equation [31, 32]:

$$\tan \delta_E = \frac{\varepsilon''}{\varepsilon'}$$

$$\tan \delta_M = \frac{\mu''}{\mu'}$$

Therefore, during the HFSS simulation process, the magnetic permeability and dielectric constant of the absorbing material are the key factors in experiment. The variable frequency permittivity and permeability data of the MXene composite used in the simulation derived from NiMR-H in [26], and its 2GHz~18GHz band parameters are shown in figure 1.

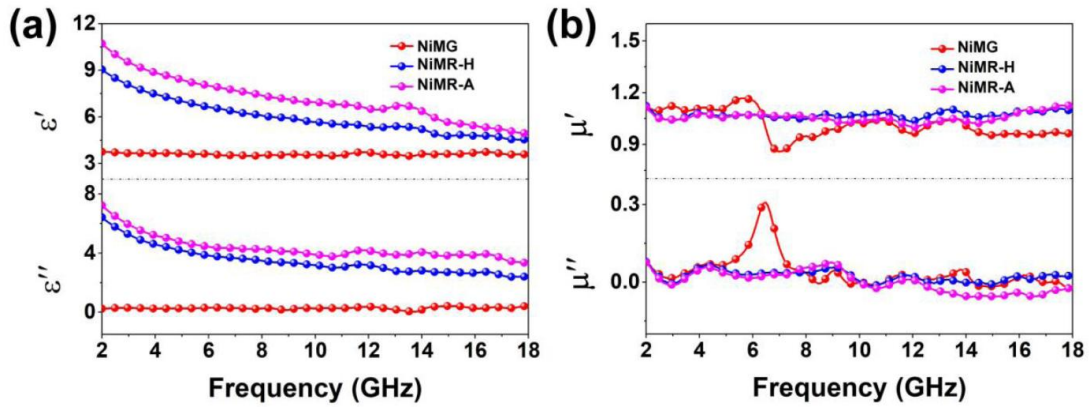

Figure 1. (a) Complex permittivity of Ni/MXene/Reduced graphene oxide (NiMR-H), and (b) complex permeability. Reprinted with permission of [26], copyright ©2021 American Chemical Society

The chassis model is cuboid, and its length, width and height are 400 mm, 300 mm and 200 mm respectively; The chassis material is 6061 aluminum alloy. The back of the chassis contains 40 mm diameter cable inlet holes and cooling windows. The heat dissipation window is composed of three independent heat dissipation windows, each of which is composed of 16 cuboids with a length, width and height of 95 mm, 1 mm and 2 mm respectively. The front of the chassis is reserved with 6*6 button windows with a length, width and height of 10.2 mm, 1 mm, and 5.2 mm. The three-dimensional structure diagram of the chassis is shown below, figure 2(a) is the three-dimensional structure diagram of the chassis, figure (2)b is the front view of the chassis, and figure 2(c) is the back view of the chassis.

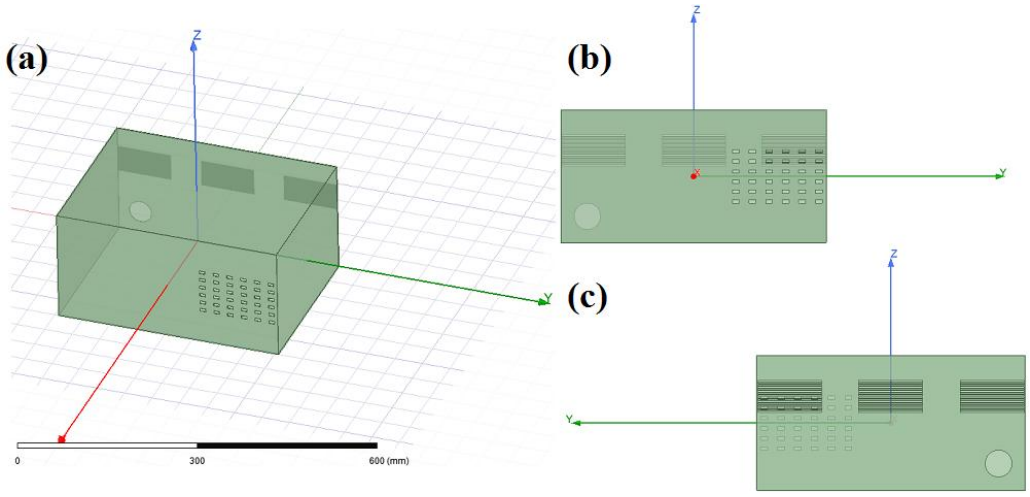

Figure 2. (a) 3D structure of the chassis, (b) front view of the chassis, (c) rear view of the chassis

The electric shielding performance can be expressed by the following equation:

$$SE_E = 20lg\left(\frac{E_0}{E_s}\right)$$

Similarly, the magnetic shielding performance can be expressed by the following equation:

$$SE_H = 20lg\left(\frac{H_0}{H_s}\right)$$

The above equation shows that in the case of the same external electromagnetic excitation source, the ratio of the corresponding field strength in the presence of shield (E_S, H_S) and the absence of shield (E_0, H_0) in the same spatial position is the shielding efficiency of the chassis equipment [33]. According to the above formula, in order to obtain the specific value of the shielding effectiveness of the chassis, it is necessary to set the excitation source externally during the simulation process and obtain the corresponding field strength size before and after adding the chassis at the same location inside the chassis. In this test, the plane wave was used as the excitation and the excitation source was placed 200 mm away from the back of the chassis, and the specific coordinates were (-350 mm, 0 mm, 0 mm); The material properties of NiMR-H were established in the HFSS material library file through the dielectric constant and magnetic permeability in figure 1. The frequency sweep was performed in the range of 2 GHz~18 GHz. Figure 3 shows the distribution of electric field strength at 10 GHz in the xoy, xoz, and yoz surfaces inside the chassis; When the excitation source is vertically polarized and horizontally polarized, the corresponding electric field maximums are 1.392 V/m and 1.410 V/m, respectively. The corresponding minimum electric field values are 0.006 V/m and 0.002 V/m, respectively. From the field strength distribution

diagram, it can be found that under the same conditions, the chassis has a better shielding effect on the excitation source of horizontal polarization than the excitation source of vertical polarization. What's more, since the original electric field amplitude of plan wave is 200 V/m, the maximum value of the electric field inside the chassis represents that the chassis has a good shielding effectiveness.

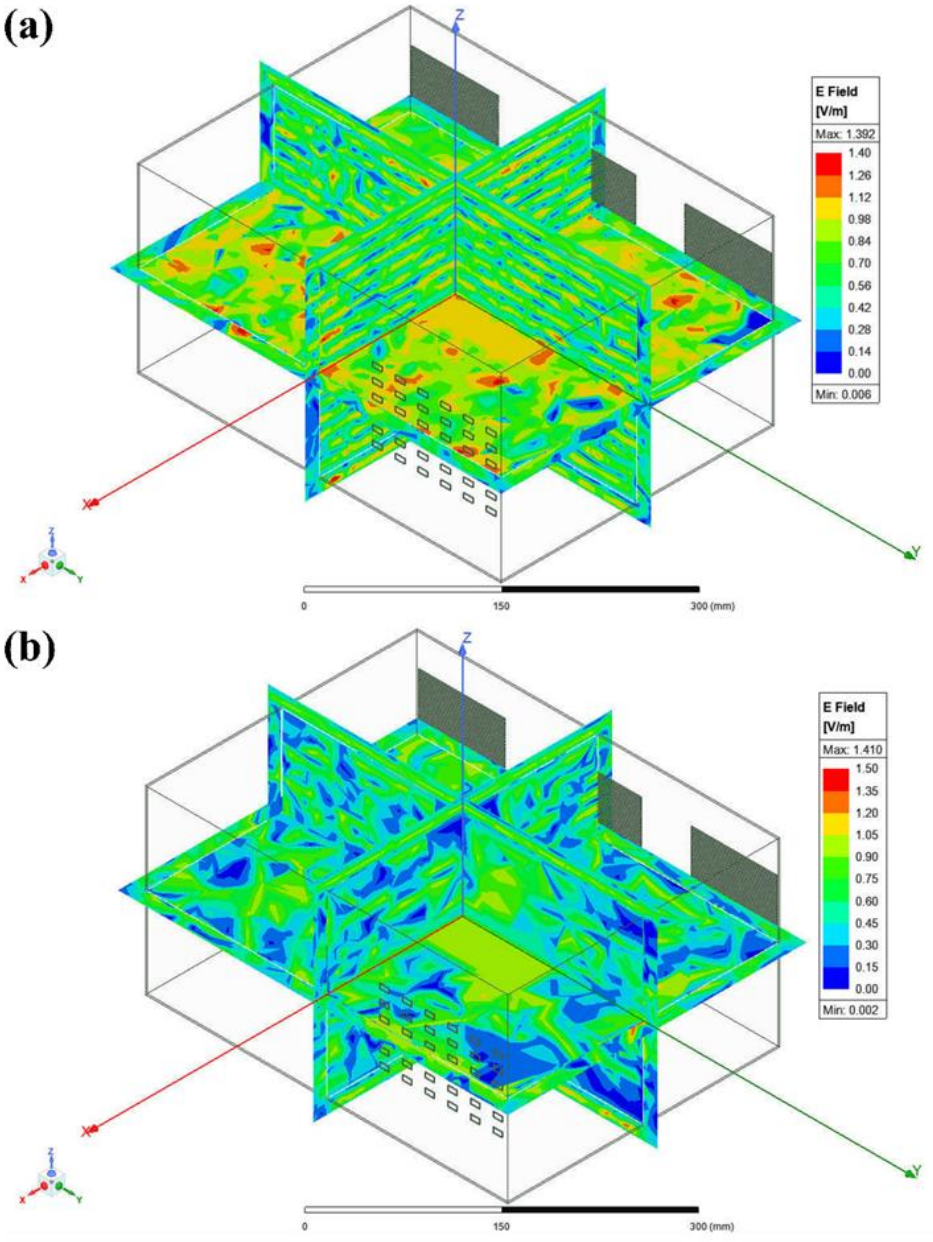

Figure 3. The electric field distribution of xoy, xoz, yoz surfaces (NiMR-H= 0 mm): (a) vertical polarization, (b) horizontal polarization

Figure 4 shows the surface current distribution on the chassis under the excitation of the external electric field. From the results of field diagram, it shows that the chassis surface has a weak induced current under vertical polarization; In the case of horizontal polarization, the

surface-induced current distribution of the chassis is narrower than the range of vertical polarization.

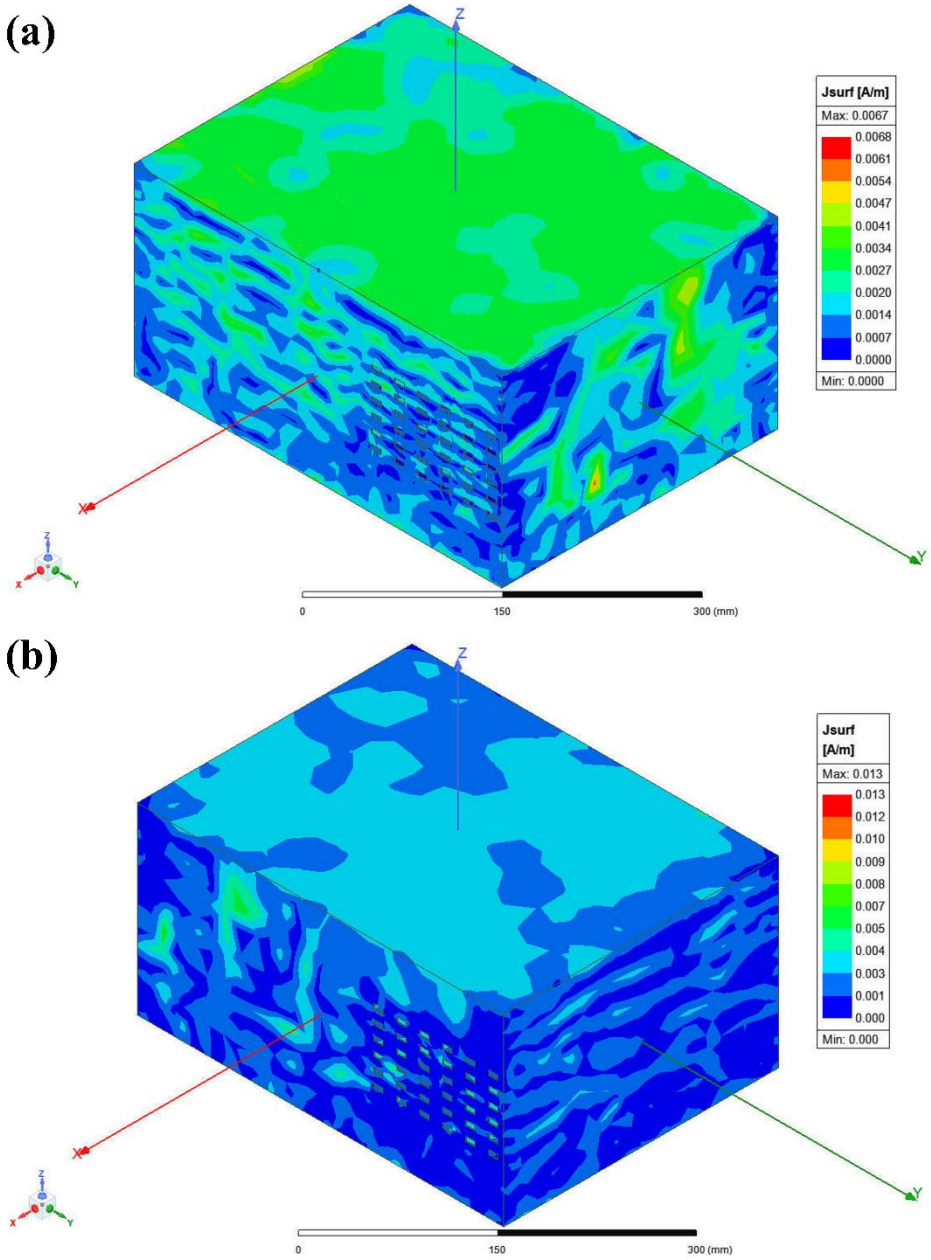

Figure 4. Current distribution on the chassis surface (NiMR-H= 0 mm): (a) vertical polarization, (b) horizontal polarization

In addition, the results of the corresponding electric and magnetic field strengths in the range of 2 GHz~18 GHz at the intersection of xoy, xoz and yoz planes (0 mm, 0 mm, 0 mm) are shown in figure 5. The amplitude of the electric field fluctuates greatly before 4 GHz, while the magnetic field has a large amplitude change before 7 GHz.

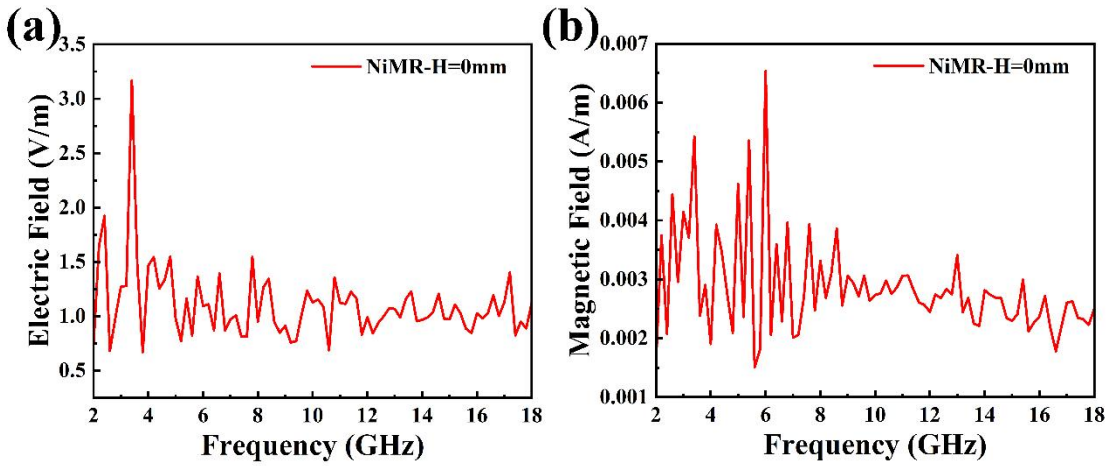

Figure 5. (a) electric field strength and (b) magnetic field strength at the origin of internal coordinates of 2GHz~18GHz chassis (NiMR-H=0 mm)

As we all know, high-frequency electromagnetic wave has a skin effect when passing through the conductor, and the specific expression of the skin effect is as follows:

$$\delta = \sqrt{\frac{1}{\pi f \mu \sigma}}$$

Where μ and σ are the magnetic permeability and conductivity of the material, respectively; f is the corresponding electromagnetic wave frequency [34]. Since electromagnetic waves have a skin effect when passing through the conductor, is it possible to use a certain thickness of absorbing material to absorb electromagnetic waves before passing through the chassis equipment to minimize the energy entering the equipment? Therefore, NiMR-H films of different thicknesses were used to cover the chassis, and the thicknesses of 0.2 mm, 0.4 mm, 0.6 mm, 0.8 mm, and 1 mm were respectively. Figure 6 is the three-dimensional model diagram of the chassis when the NiMR-H film thickness is 0.2 mm, and the chassis model of 0.4 mm~1 mm is extrapolated on this basis.

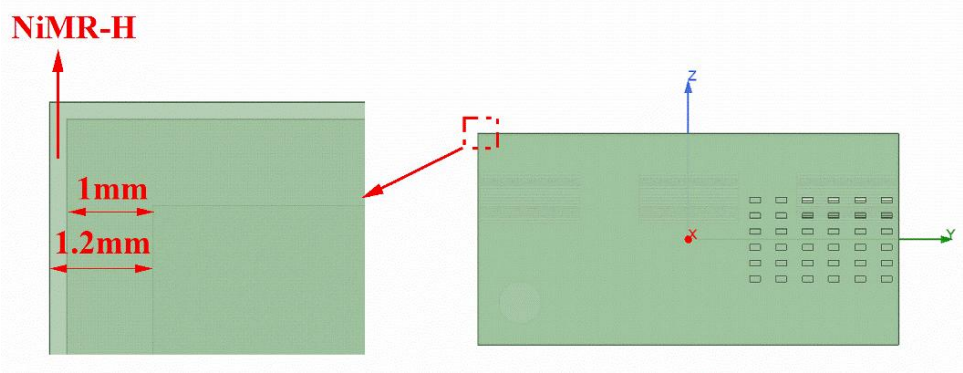

Figure 6. 3D chassis model of 0.2 mm thick MXene composite material

As shown in figure 7, with the gradual increase of the thickness of MXene matrix composite, the electric field inside the chassis at the origin under the irradiation of vertical polarization waves shows a trend of first decreasing and then increasing. When the thickness is 0.6mm, the corresponding electric field value at the origin is the lowest.

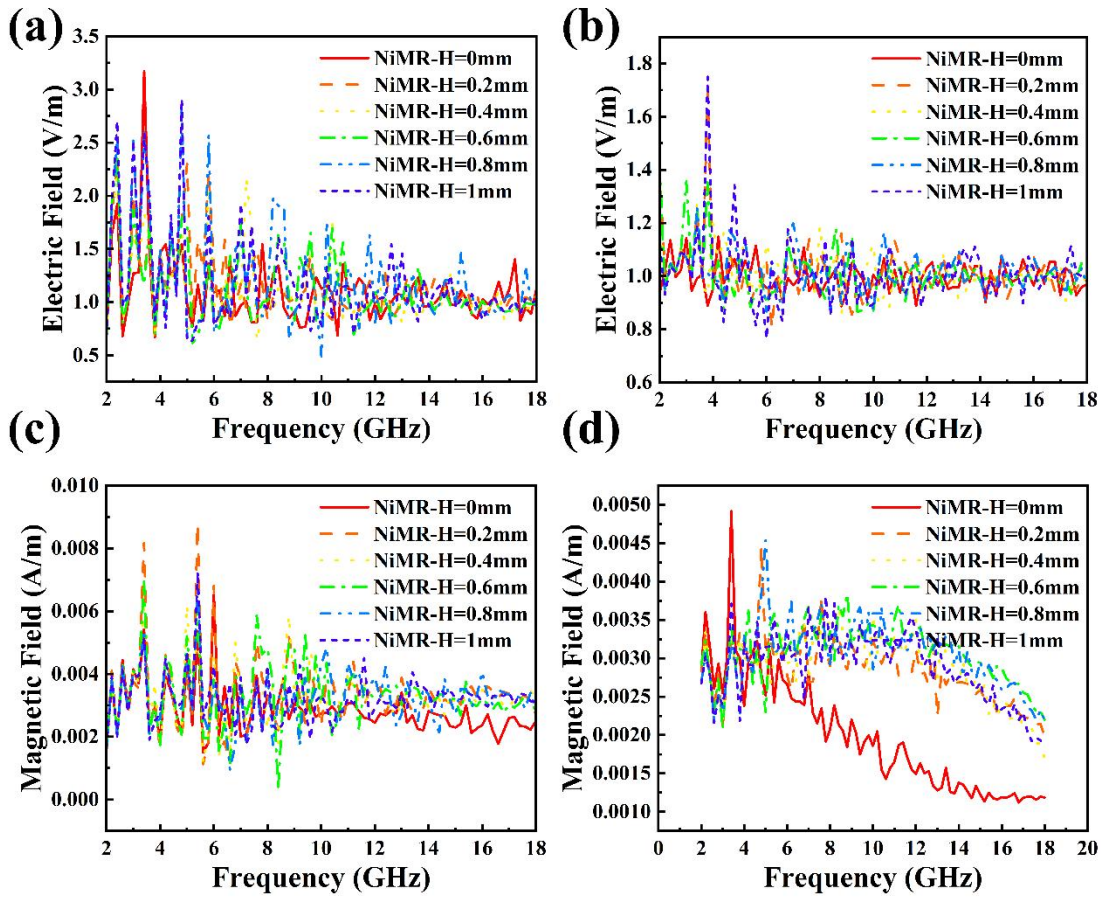

Figure 7. The electric field strength under vertical polarization at the origin (a) when the thickness of the composite is 0mm, 0.2mm, 0.4mm, 0.6mm, 0.8mm and 1mm; (b) The strength of the electric field at horizontal polarization; (c) Magnetic field strength under vertical polarization; (d) The strength of the magnetic field at horizontal polarization

Materials with core-shell, core-sheath, yolk-shell and other similar three-dimensional structures have been widely used in the construction of electromagnetic absorbing materials. Since NiMR-H also has a three-dimensional structure with a large specific surface area, it is beneficial for improving the absorption performance of the material [24, 26]; In addition, the Ni element in the composite material can adjust the impedance matching effect of the composite in the high-frequency band and the corresponding microwave loss [23].

4 Conclusions

In this paper, HFSS is used to simulate the shielding efficiency of the chassis, and the simulation results show that when the chassis surface is optimized by NiMR-H composite, the amplitude value of the electric field inside the chassis decreases with the gradual increase of the thickness of the absorbing material. When the thickness of the composite material is 0.6mm, it has the most considerable shielding effect; As the thickness of the absorbing material further increases, the induced voltage value at the internal origin of the chassis gradually increases. In summary, similar absorbing materials can be used in the process of improving the radiated immunity of similar equipment in order to optimally complete the electromagnetic compatibility performance of the device.

Acknowledgements

This work was supported by the Guangzhou GRG Metrology & Test Co., Ltd.

References

[1] Wang, Z., Cheng, Z., Fang, C. Q., Hou, X. L., Xie, L., “Recent advances in MXenes composites for electromagnetic interference shielding and microwave absorption,” Composites, Part A, 136. 105956. Sept.2020.

[2] Liang, L. Y., Yang, R. S., Han, G. J., Feng, Y. Z., Zhao, B., Zhang, R., Wang, Y. M., Liu, C. T., “Enhanced Electromagnetic Wave-Absorbing Performance of Magnetic Nanoparticles-Anchored 2D Ti3C2Tx MXene, ” ACS Appl. Mater. Interfaces, 12(2). 2644-2654. Dec.2020.

[3] Cao, M. S., Wang, X. X., Zhang, M., Shu, J. C., Cao, W. Q., Yang, H. J., Fang, X. Y., Yuan, J., “Electromagnetic Response and Energy Conversion for Functions and Devices in Low-Dimensional Materials,” Adv. Funct. Mater., 29(25). 1807398. Jun.(2019).

[4] Xu, H. L., Yin, X. W., Li, X. L., Li, M. H., Liang, S., Zhang, L. T., Cheng, L. F., “Lightweight Ti2CTx MXene/Poly(vinyl alcohol) Composites Foams for Electromagnetic Wave Shielding with Absorption-Dominated Feature,” ACS Appl. Mater. Interfaces, 11(10). 10198-10207. Jan.2019.

[5] Alam, S. M. J., Alam, M. R., Hu, G. Q., Mehrab, M. Z., “Bit Error Rate Optimization in Fiber Optic Communications,” Int. J. Mach. Learn. Comput., 1(5). 435-440. Dec.2011.

[6] Aldossari, S. M., Chen, K. C., “Machine Learning for Wireless Communication Channel Modeling: An Overview,” Wireless Pers Commun, 106. 41-70.Mar.2019.

[7] Hunt, B. J., “Oliver Heaviside: A first-rate oddity,” Phys. Today 64(11). 48-53. Nov.2012.

[8] Wu, J. H., Scholvin, J., del Alamo, J. A., Jenkins, K. A., “A faraday cage isolation structure for substrate crosstalk suppression,” IEEE Micro Wire CO., 11(10). Oct.410-412.2001.

[9] H. B. Liu, R. L. Fu, X. Q. Su, X. D. Chen, B. Y. Wu, Mxene Structure, Properties and Application in the Filed of Electromagnetic Shielding, Mater. Rep. 35, 13067-13074(2021).

[10] Chung, D. D. L., “Materials for electromagnetic interference shielding,” Mater. Chem. Phys,. 255, 123587. Nov.2020.

[11] Dai, B., Ma, Y., Dong, F., Yu, J., Ma, M. L., Thabet, H. K., El-Bahy, S. M., lbrahim, M. M., Huang, M., Seok, l., Roymahapatra, G., Naik, N., Xu, B. B., Ding, J. X., Li, T. X., “Overview of MXene and conducting polymer matrix composites for electromagnetic wave absorption,” Adv. Compos. Hybrid Mater., 5. 704-754. Jul.2022.

[12] Naguib, M., Kurtoglu, M., Presser, V., Lu, J., Niu, J. J., Heon, M., Hultman, L., Gogotsi, Y., Barsoum, M. W., “Two-Dimensional Nanocrystals Produced by Exfoliation of Ti3AlC2,” Adv. Mater., 23(37). 4248-4253. Oct.2011.

[13] Deng, Q. H., Feng, Y. F., Li, W., Xu, X. Q., Peng, C., Wu, Q., “Strong interface effect induced high-k property in polymer based ternary composites filled with 2D layered Ti3C2 MXene nanosheets,” J. Mater: Mater in Electron, 30. 9106-9113.Mar.2019.

[14] Shuck, C. E., Sarycheva, A., Anayee, M., Levitt, A., Zhu, Y. Z., Uzun, S., Balitskiy, V., Zahorodna, V., Gogotsi, O., Gotosi, Y., “Scalable Synthesis of Ti3C2Tx MXene,” Adv. Eng. Mater., 22(3). 1901241. Mar.2020.

[15] Kim, H., Alshareef, H. N., “MXetronics: MXene-Enabled Electronic and Photonic Devices,” ACS Mater. Lett., 2(1). 55-70. Nov.2020.

[16] Ma, C., Ma, M. G., Si, C. L., Ji, X. X., Wan, P. B., “Flexible MXene-Based Composites for wearable Devices,” Adv. Funct. Mater. 31(22). 2009524.May.2021.

[17] Rasool, K., Helal, M., Ali, A., Ren, C. E., Gotosi, Y., Mahmoud, K. A., “Antibacterial Activity of Ti3C2Tx MXene,” ACS Nano, 10(3). 3674-3684.Feb.2016.

[18] Kuang, P. Y., Low, J. X., Cheng, B., Yu, J. G., Fan, J. J., “MXene-based photocatalysts,” J. Mater. Sci. Technol., 56. 18-44.Nov.2020.

[19] Hu, M. M., Zhang, H., Hu, T., Fan, B. B., Wang, X. H., Li, Z. J., "Emerging 2D MXenes for supercapacitors: status, challenges and prospects," Chem. Soc. Rev., 49(18). 6666-6693.Aug.2020.

[20] Leong, C. C., Qu, Y. J., Kawazone, Y., Ho, S. K., Pan, H., "MXenes: Novel electrocatalysts for hydrogen production and nitrogen reduction," Catal. Today, 370. 2-13.Jun.2021.

[21] Mirkhani, S. A., Zeraati, A. S., Aliabadian, E., Naguib, M., Sundararaj, U., "High dielectric constant and low dielectric loss via poly(vinylalcohol)/Ti3C2Tx MXene Nanocomposites," ACS Appl. Mater. Interfaces, 11(2). 18599-18608.Nov.2019.

[22] Meng, K., Li, W. H., Tang, X. G., Liu, Q. X., Jiang, Y. P., "The defect related energy-storage properties of A-site off-stoichiometry ferroelectric ceramic," Appl. Phys. A, 337. 127.Apr.2021.

[23] Wu, M., Rao, L., Zhang, J. F., Li, Y. X., Ji, Z. Y., Ying, G. B., "Research progress in preparation and performance of MXene and its composites absorbing materials," J. Compos. Mater., 39(3). 942-955.Mar.2022.

[24] Zhang, Z. W., Cai, Z. H., Zhang, Y., Peng, Y. L., Wang, Z. Y., Xia, L., Ma, S. P., Yin, Z. Z., Wang, R. F., Cao, Y. S., Li, Z., Huang, Y., "The recent progress of MXene-Based microwave absorption materials," Carbon, 174. 484-499.Apr.2021.

[25] Wang, T., Chen, G., Zhu, J. H., Gong, H., Zhang, L. M., Wu, H. J., "Deep understanding of impedance matching and quarter wavelength theory in electromagnetic wave absorption," J. Colloid Interface Sci., 595. 1-5.Aug.2021.

[26] Liang, L. Y., Li, Q. M., Yan, X., Feng, Y. Z., Wang, Y. M., Zhang, H. B., Zhou, X. P., Liu, C. T., Shen, C. Y., Xie, X. L., "Multifunctional magnetic Ti3C2Tx MXene/Graphene aerogel with superior electromagnetic wave absorption performance," ACS Nano, 15(4). 6622-6632.Mar. 2021.

[27] Wu, N. N., Xu, D. M., Wang, Z., Wang, F. L., Liu, J. R., Liu, W., Shao, Q., Liu, H., Gao, Q., Gao, Z. H., "Achieving superior electromagnetic wave absorbers through the novel metal-organic frameworks derived magnetic porous nanorods," Carbon, 145. 433-444.Apr.2019.

[28] Liu, P. B., Zhang, Y. Q., Yan, J., Huang, Y., Xia, L., Guang, Z. X. "Synthesis of lightweight N-doped graphene foams with open reticular structure for high-efficiency electromagnetic wave absorption," Chem. Eng. J., 368. 285-298.Jul.2019.

[29] Qiu, Y., Lin, Y., Yang, H.B., Wang, L., Wang, M. Q., Wen, B., "Hollow Ni/C microspheres derived from Ni-metal organic framework for electromagnetic wave absorption," Chem. Eng. J., 383.123207.Mar.2020.

[30] Zeng, M., Cao, Q., Liu, J., Guo, B. Y., Hao, X. Z., Liu, Q. W., Sun, X., Zhang, X. X., Yu, R. H., "Hierarchical Cobalt Selenides as highly efficient microwave absorbers with tunable Frequency Response," ACS Appl. Mater. Interfaces, 12(1).1222-1231.Dec.2020.

[31] Wang, C., Han, X. J., Xu, P., Zhang, X. L., Du, Y. C., Hu, S. R., Wang, J. Y., Wang, X. H., "The electromagnetic property of chemically reduced graphene oxide and its application as microwave absorbing material," Appl. Phys. Lett., 98(7), 072906.Feb.2011.

[32] Cao, M. S., Yang, J., Song, W. L., Zhang, D. Q., Wen, B., Jin, H. B., Hou, Z. L., Yuan, J., "Ferroferric Oxide/Multiwalled Carbon Nanotube vs Polyaniline/Ferroferric Oxide/Multiwalled Carbon Nanotube Multiheterostructures for Highly Effective Microwave Absorption," ACS Appl. Mater. Interfaces, 4(12). 6949-6956.Nov.2012.

[33] Marvin, A. C., Dawson, J. F., Ward, S., Dawson, L., Clegg, J., Weissenfeld, A., "A proposed new definition and measurement of the shielding effect of equipment enclosures," IEEE Trans. Electromag. Compat., 46(3). 459-468.Aug.2004.

[34] Wheeler, H. A., "Formulas for the skin effect," Proc. IRE, 30(9). 412-424.Sept.1942.